Attributes Assisted Seismic Interpretation in Pre-Stack Time versus Depth Migration Data*

Tengfei Lin[1], Hang Deng[1], Zhifa Zhan[2], Zhonghong Wan[2], and Kurt Marfurt[1]

Search and Discovery Article #41637 (2015)
Posted June 30, 2015

*Adapted from extended abstract prepared in conjunction with oral presentation at AAPG Annual Convention & Exhibition 2015, Denver, Colorado, May 31-June 3, 2015.

[1] School of Geology and Geophysics, University of Oklahoma, Norman, Oklahoma, United States (tengfei.lin@ou.edu)
[2] BGP Inc., CNPC, Zhuozhou, Hebei, China

Abstract

Pre-stack time migration (PSTM) has pitfalls in processing seismic data, which causes artificial features on seismic images and might mislead the structural interpretation. First, fault shadows give rise to a second (artificial) discontinuity coherence images computed from PSTM data. Second, velocity pull-up and push-down caused by the lateral changes in the overburden such as carbonate buildups and incised valleys will give rise to erroneous curvature anomalies in PSTM data. Besides, PSTM data may be poorly focused in complex structures. Fault terminations of reflectors may be misaligned, giving rise to “wormy” coherence anomalies. Channels and other stratigraphic features may be diffused, making them hard to interpret. To remove the above pitfalls caused by PSTM, pre-stack depth migration (PSDM), which assumes that seismic waves are propagated in straight rays, is necessary in the presence of strong lateral velocity variation to avoid these artifacts. The more accurate velocity model established by PSDM better images complex structures. The seismic data from the Bohai Bay Basin in China are separately processed by PSTM as well as PSDM, combining with seismic attributes, to compare the seismic imaging quality. Several sub-fault splays artifacts in coherence generate the fault-shadow zones under dipping main faults in PSTM data, but disappear in PSDM data. The curvature anomalies related to the lateral variations may be misinterpreted as real structures in PSTM data, which are removed in precise velocity PSDM data. Therefore, In the presence of strong lateral variations in velocity, PSDM is better for interpreting complex structures comparing PSTM which fails to properly image the subsurface. This study aims at illustrating the pitfalls in the seismic interpretation. Considering lateral velocity variations, conventional time migration data has some pitfalls, which may lead to misinterpretation. Depth migration data possesses a more precise velocity model and can remove or suppress the velocity-related artifacts.

Introduction

Coherence algorithms measure lateral variations in seismic waveform (Bahorich and Farmer, 1995, 1996). Similar with other attributes, coherence is sensitive to noise. To avoid this problem, Kirlin (1992), Marfurt et al. (1998), and Gersztenkorm and Marfurt (1996, 1999) introduce more robust multi-trace semblance- and eigenstructure-based coherence algorithms, which improve imaging in the presence of random noise.

In contrast to random noise, all coherence algorithms are sensitive to fault shadows in time migration data. Fagin (1991) uses forward ray trace modeling to illustrate the fault shadow problem. A more complete description of the “fault whisper” problem on prestack data is given by Hatchell (2000). Fault whisper is the phenomenon of transmission distortions, which are produced by velocity variations across buried faults and unconformities and related to the phenomenon known as fault shadows.

Depth migration data presents its own challenges. In time migration, the major impact of velocity is to focus or defocus reflectors and diffractors with some lateral movements. In depth migration, these features are also moved laterally and vertically. If the velocity model is inaccurate, depth migration may be inferior to time migration. Even though the data are properly imaged, the wavelet spectrum is no longer in Hertz, but in wavenumber, which decreases as velocity increases with depth.

Methodology

For the Kirchhoff prestack time migration (PSTM), the total traveltime t is the sum of source to scatter point time and the scatter point to receiver time t_r (see Figure 1):

$$\boldsymbol{t = t_s + t_r} \tag{1}$$

Assuming that the velocity **v** is constant, equation 1 can be expanded to:

$$t = \left[\frac{h_0^2 + (x + l)^2}{V^2}\right]^{\frac{1}{2}} + \left[\frac{h_0^2 + (x - l)^2}{V^2}\right]^{\frac{1}{2}} \tag{2}$$

where $\boldsymbol{h_0}$ is the depth of the scatter point, $\boldsymbol{x}$ is the location of the source-receiver midpoint (MP), and $\boldsymbol{h}$ is half of the source-receiver offset.

Considering that:

$$t_0 = \frac{2h_0}{V_{avg}} \tag{3}$$

where $\boldsymbol{V_{avg}}$ is the average velocity for the two-way zero-offset time.

Therefore, equation 2 can be modified to:

$$t = \left[\left(\frac{t_0}{2}\right)^2 + \frac{(x+l)^2}{V_{rms}^2}\right]^{\frac{1}{2}} + \left[\left(\frac{t_0}{2}\right)^2 + \frac{(x+l)^2}{V_{rms}^2}\right]^{\frac{1}{2}} \tag{4}$$

where $\boldsymbol{V_{rms}}$ is the migration velocity, which is approximate to the RMS velocity for the horizontal “cake” model.

Pitfalls

Figure 2 indicates a fault model as well as its PSTM seismic profile. Two high velocity zones are set into the model, which are marked as purple- and green- colored layers. Figure 3 shows in detail of these oscillations, point A-H are the points located at the main fault of the model. The semi-transparent yellow-colored zone indicates the fault shadow, which is intensively distorted compared to the structural model. For high velocity zone 1, the push-down is marked between point A and B, and the pull-up is marked between point B and D. For high velocity zone 2, the push-down is marked between point F and G. In Figure 3, near-vertical structural axes (red solid lines) can be drawn which link the positions of these anomalies for each underlying reflection. These axes are predictable consequences of extensional faulting in the study area. In the real data example presented later, they are shown to occur in each fault block (Fagin, 1991). Both the push-down and pull-up phenomenon are the time anomalies, which can be explained using zero-offset two-way travel time. The push-down will generate trough, because of the slower traveltime; while the pull-up will generate crest because of the faster traveltime.

Figure 4 is the seismic profile of PSTM amplitude volumes. In Figure 4, F1 and F2 are two major faults, and H1-H5 are horizons. The seismic pitfall (pull-up) is indicated by the red arrow, which is caused by the existence of high velocity zone between H3 and H5. The structural high zone (yellow-colored shadow) seems unreasonable. This is because it is at upthrow, which means they should be structural low zone.

Coherence is an important aid in fault interpretation. Figure 5 indicates the vertical slice though coherence co-rendered with seismic amplitude of Figure 4. The grey curved solid line indicated by grey arrow ban is interpreted as sub-fault splays to the main fault F2.

The most-positive curvature and most-negative curvature are co-rendered with seismic amplitude of time migration and depth migration data in Figure 6. The blue zones indicated by blue arrows for faults F2 and F3 are interpreted to be synclines with most negative curvature, while the red zones indicated by red arrows are interpreted to be anticlines with most positive curvature. Considering the faults F2 and F3 are normal faults, the parallel most positive- and negative- curvature seems unreasonable.

Figure 7 indicates the vertical slice though peak frequency co-rendered with seismic amplitude (Figure 4) for PSTM data. The high velocity zone is marked by the black arrow between horizon H3 and H4, with a peak frequency of about 30 Hz and will be wider in depth than in time domain. The white arrow indicates the zone between horizon H4 and H5, with a peak frequency of about 20Hz.

Mitigation

Figure 8 indicates that the seismic profile of the prestack Kirchhoff depth migration seismic data (PSDM) perfectly matches the fault model except for the tiny zone indicated by the red arrow. The pitfalls (pull-up and push-down) in Figure 3 are suppressed in Figure 8 compared to the PSTM data shown in Figure 3.

Examining the real data, we note that Figure 9 can more accurately describe the structure than Figure 4. The pull-up indicated by the red arrow as well as the fault shadow in Figure 4 disappear in Figure 9. The PSTM fault shadow can be misinterpreted as sub-fault splays to the main fault F2 in Figure 5. Figure 10 shows the corresponding vertical slice though coherence co-rendered with seismic amplitude for PSDM data. Note the sub-fault “splay” artifacts are suppressed. Figure 11 shows the corresponding vertical slice though most positive curvature co-rendered with most negative curvature (with long wavelength) and seismic amplitude. The parallel synclinal and anticlinal velocity push-down and pull-up artifacts indicated by blue and red arrows in Figure 6 disappear in Figure 11. Figure 12 shows the vertical slice though peak frequency co-rendered with seismic amplitude for PSDM data. We can found that the peak frequency in the time domain is about twice for the peak wavenumber in the depth domain. Black and white arrows in Figure 12 indicate the corresponding zones in Figure 7 where the peak wavenumber is 13 cycles/km in Figure 12 vs. 30 cycles/s in Figure 7. This apparent decrease in wavenumber with depth is due to the high velocity zone indicated by the black arrow,

Conclusions

In general, depth migration is necessary in the presence of strong lateral velocity variation and avoids some of pitfalls that occur in time migration data (see Table 1). First, fault shadows can give rise to a second (artificial) discontinuity coherence images computed from PSTM data. Such artifacts are removed in accurate velocity PSDM data. Second, velocity pull-up and push-down caused by the lateral changes of the overburden such as carbonate buildups and incised valleys will give rise to erroneous curvature anomalies in time migration data. These artifacts disappear in properly depth migration data. Third, in complex structure PSTM data may be poorly focused. Fault terminations of reflectors may be misaligned, giving rise to “wormy” coherence anomalies. Channel and other stratigraphic features may be diffused, which increases the difficulties of interpretation.

Acknowledgements

We thank the sponsors of the OU Attribute-Assisted Seismic Processing and Interpretation Consortium (AASPI) and their financial support, as well as the support from The Institute of Reservoir Characterization (IRC). We thank BGP Inc., for providing the seismic data and their permission to publish. Software is provided by Tesseral Technology Inc., and Schlumberger Limited. ConocoPhillips School of Geology and Geophysics at the University of Oklahoma is thanked for the I.T. support.

References Cited

Bahorich, M.S., and S.L. Farmer, 1995, 3-D seismic discontinuity for faults and stratigraphic features: The Leading Edge, v. 14, p. 1053–1058.

Bahorich, M.S., and S.L. Farmer, 1996, Methods of seismic signal processing and exploration: U.S. Patent 5 563 949.

Fagin, S.W., 1991, Seismic modeling of geologic structures: Applications to exploration problems: Geophysical Development series, 2. Society of Exploration Geophysics.

Gersztenkorm, A., and K.J. Marfurt, 1996, Eigenstructure based coherence computations: 66th Annual International Meeting, SEG, Expanded Abstracts, p. 328-331.

Gersztenkorm, A., and K.J. Marfurt, 1999, Eigensturcture based coherence computations as an aid to 3-D structural and stratigraphic mapping: Geophysics, v. 64, p. 1468-1479.

Hatchell P.J., 2000, Fault whispers: Transmission distortions on prestack seismic reflection data: Geophysics, v. 65, p. 377–389.

Kirlin, R., 1992, The relationship between semblance and eigenstructure velocity estimators: Geophysics, v. 57, p. 1027-1033.

Marfurt, K.J., R.L. Kirlin, S.H. Farmer, and M.S. Bahorich, 1998, 3-D seismic attributes using a running window semblance-based coherency algorithm: Geophysics, v. 63, p. 1150-1165.

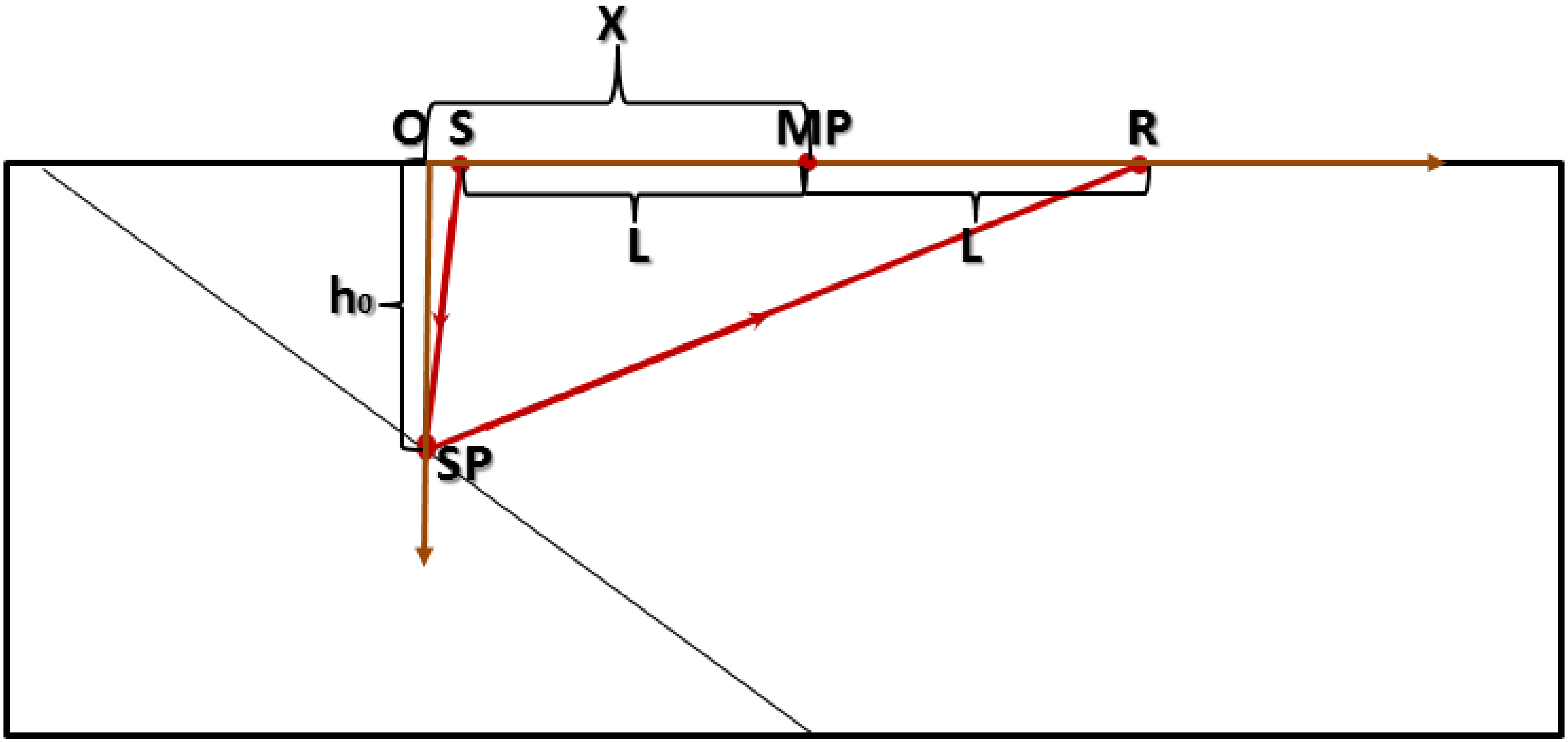

Figure 1. The geometry of PSTM. S: Source, R: Receiver, MP: Midpoint of the source and receiver, SP: Scatter point of sub-surface; X: the distance between point O and MP, L: the distance source and midpoint as well as midpoint and receiver. h_0: the depth of the scatter point.

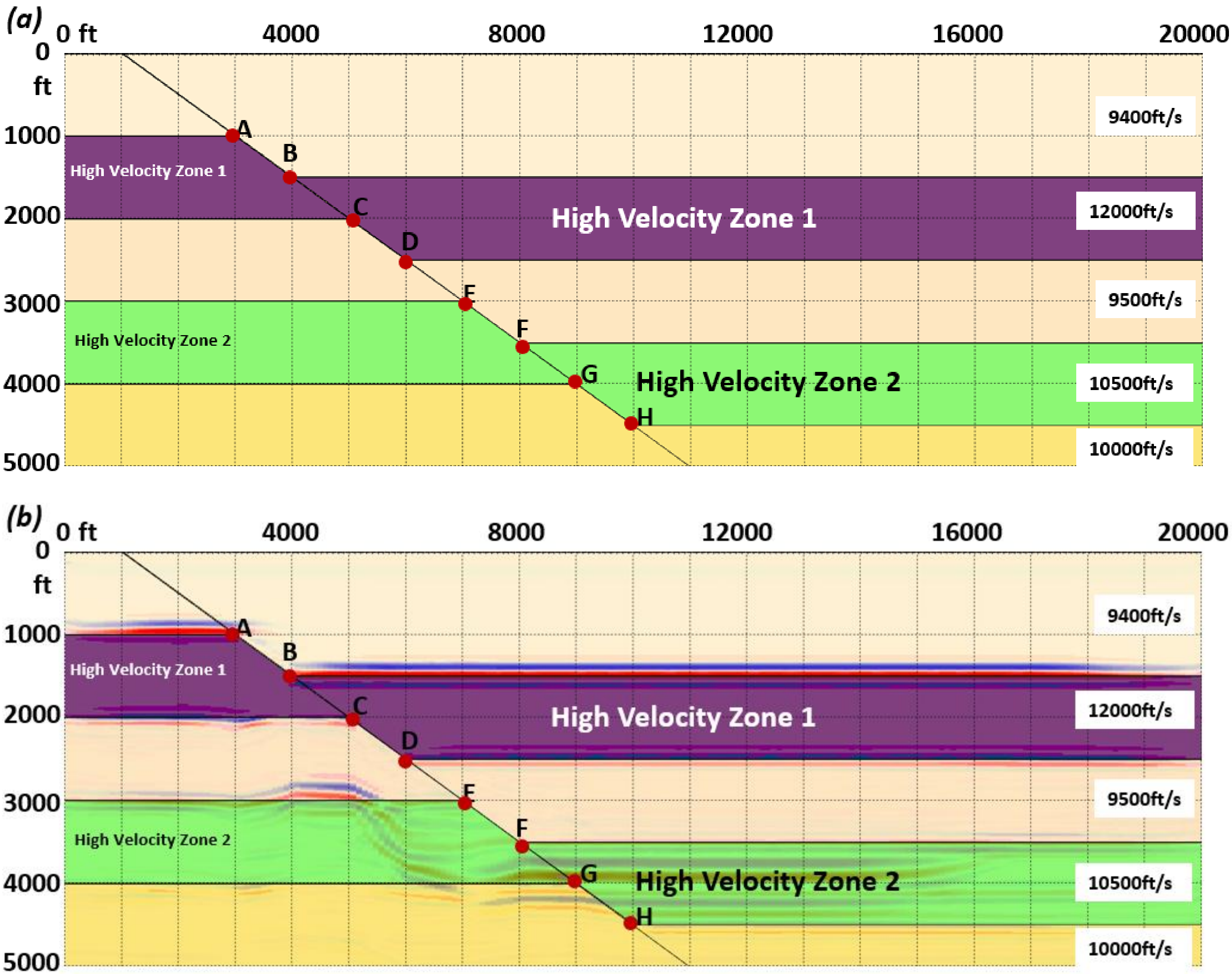

Figure 2. (a) The fault model; (b) the PSTM seismic profile of (a).

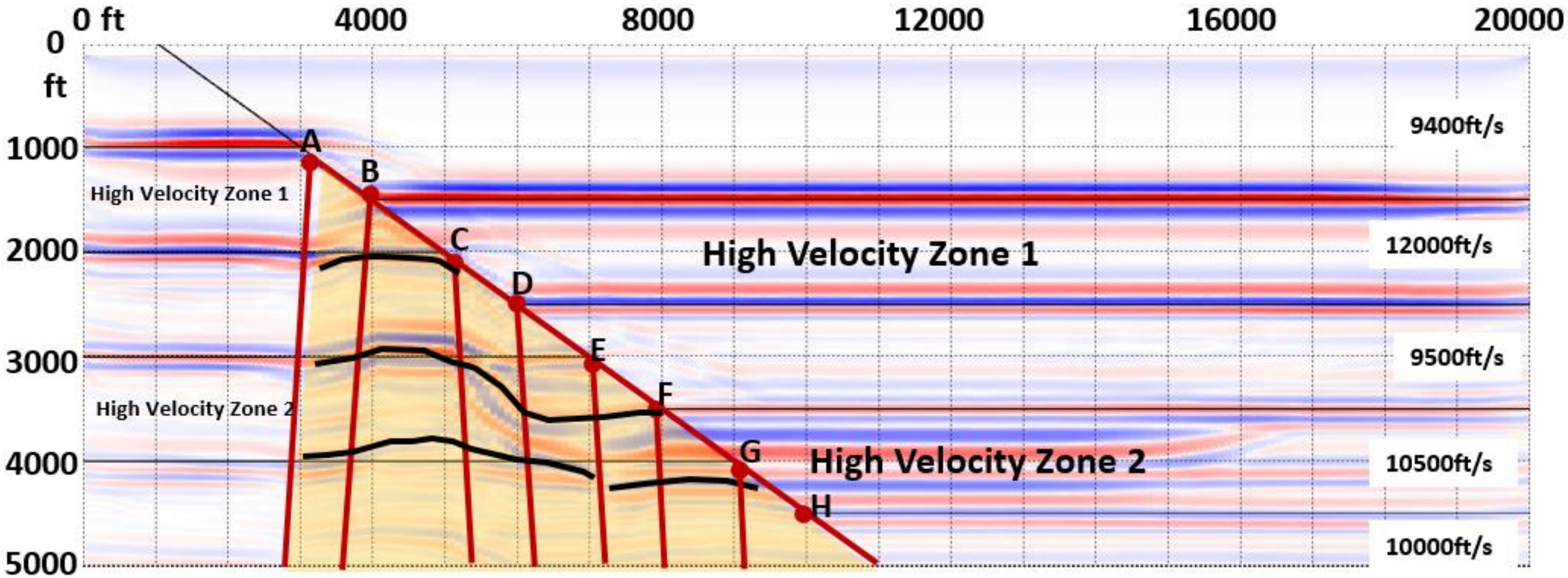

Figure 3. The PSTM seismic profile of the fault model.

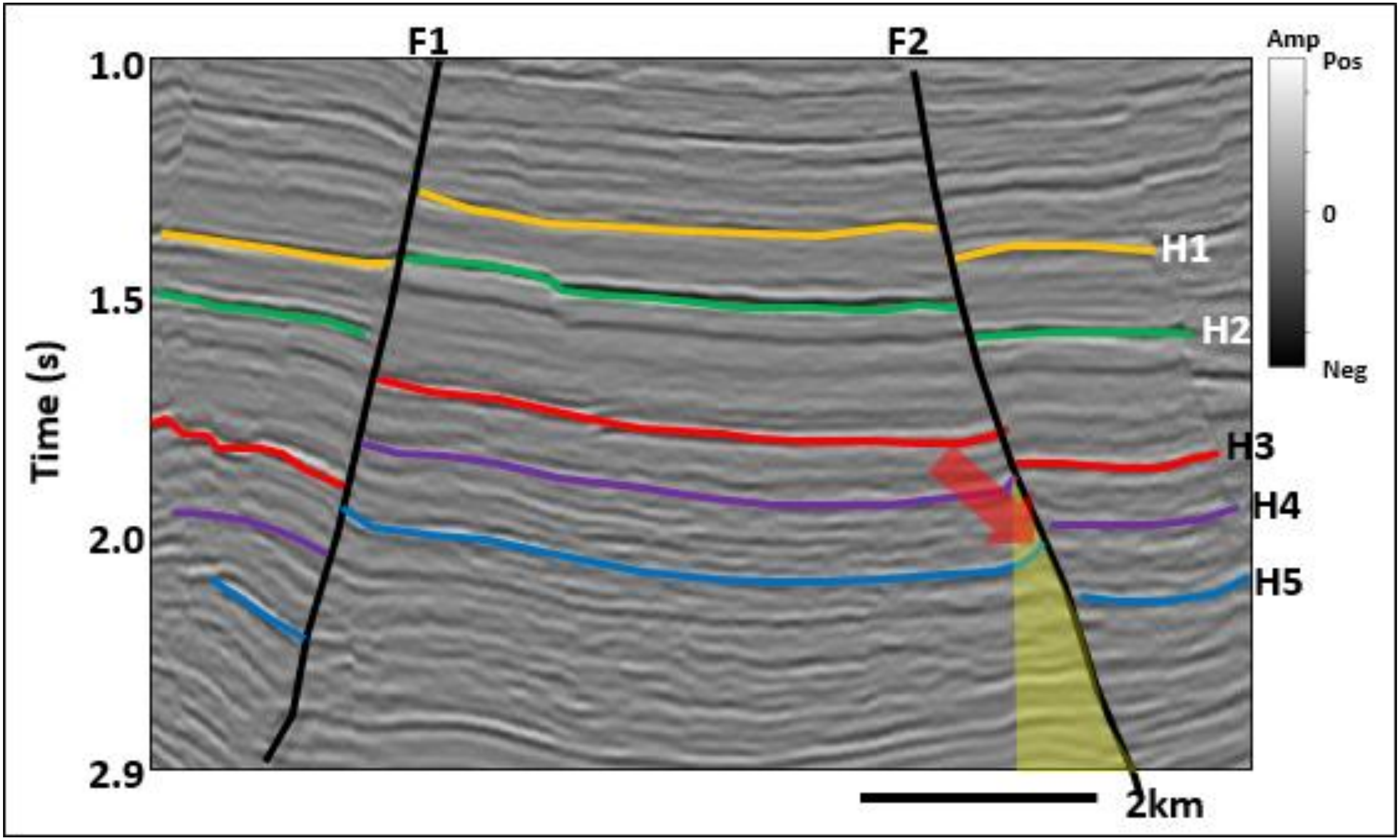

Figure 4. Seismic profile of PSTM amplitude volumes. The survey is located in Hebei Province, which was acquired by BGP Inc, China National Petroleum Corporation.

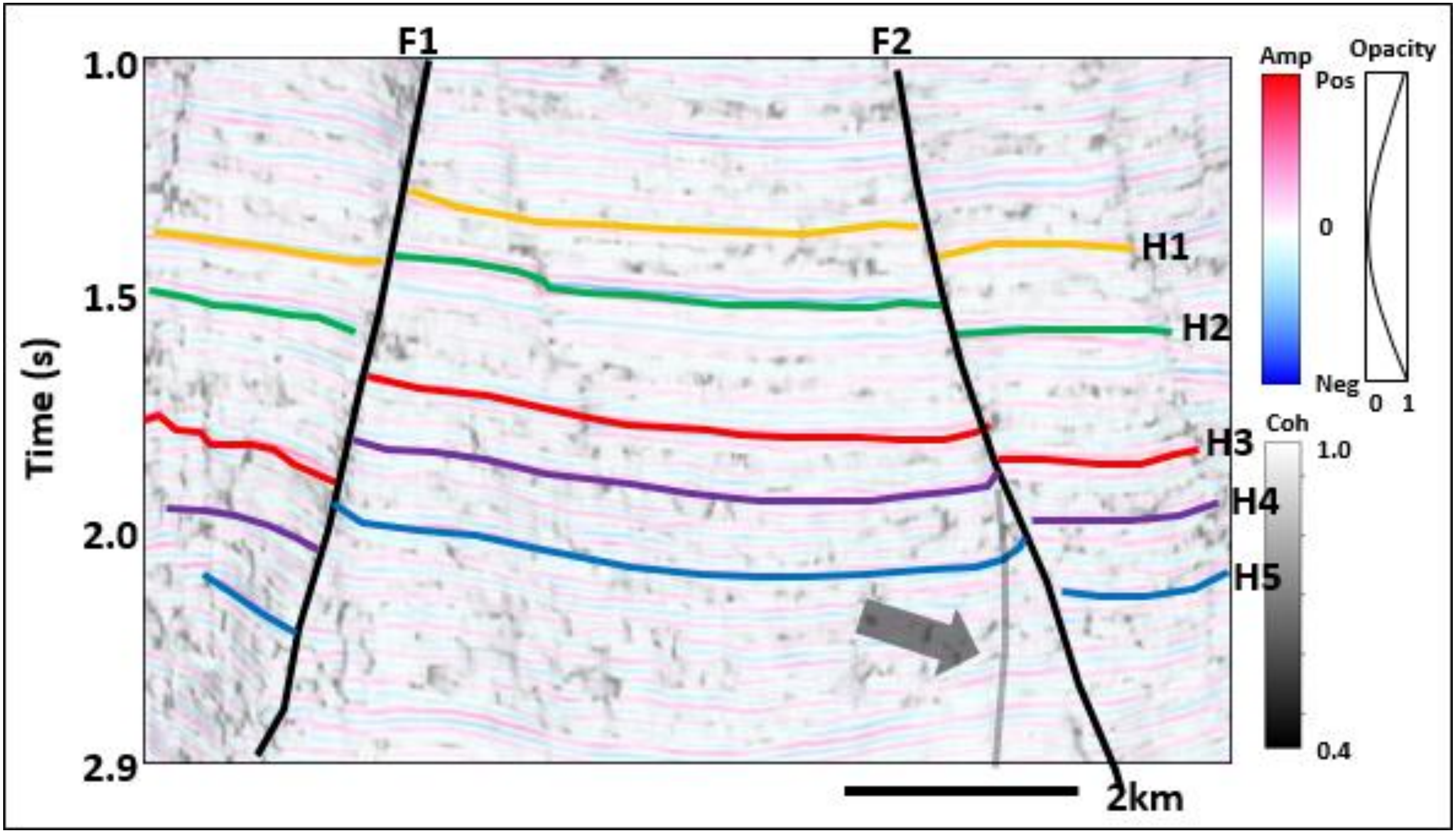

Figure 5. Vertical slice though coherence co-rendered with seismic amplitude for PSTM data.

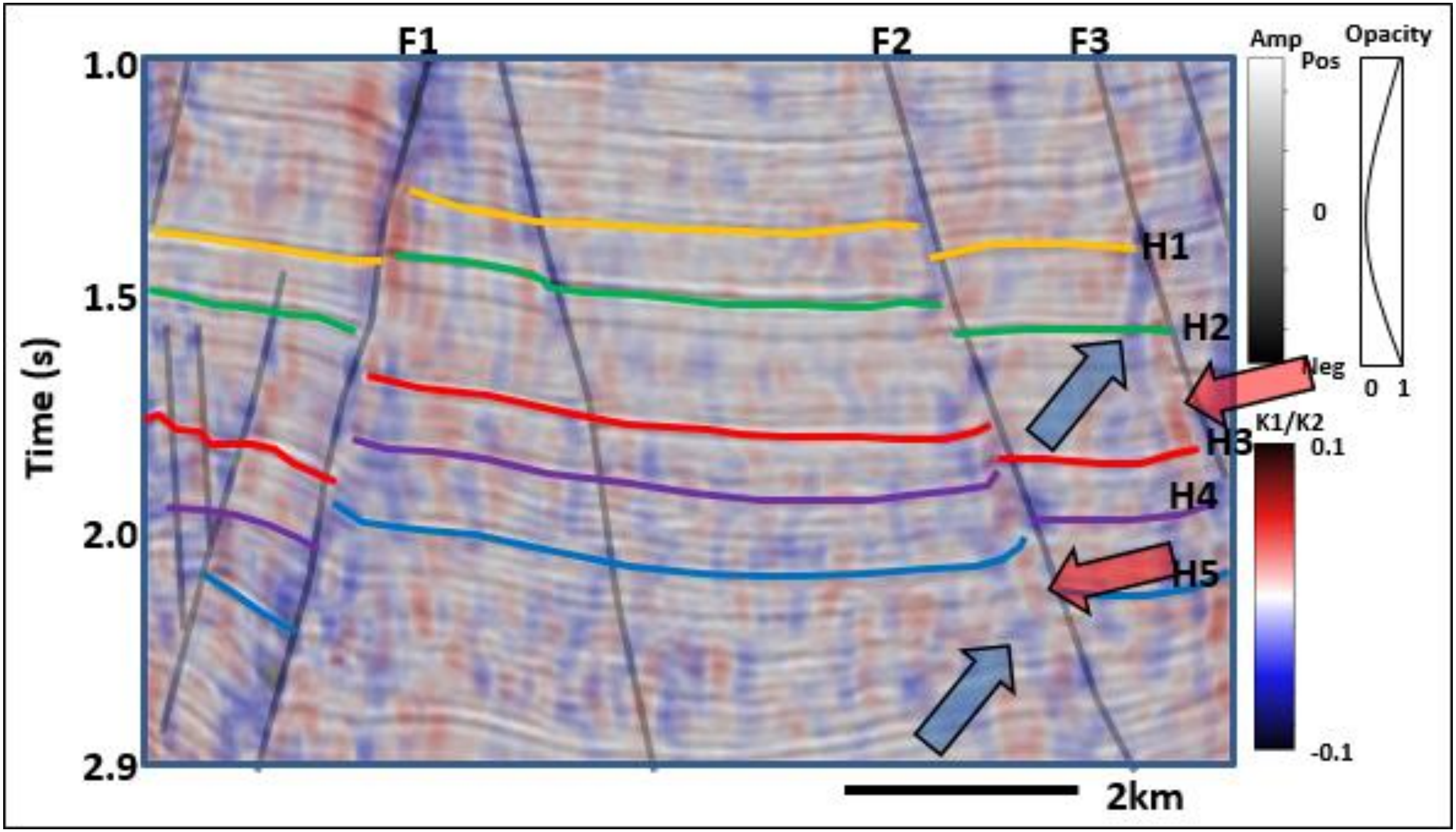

Figure 6. Vertical slice though most positive curvature co-rendered with most negative curvature (with long wavelength) and seismic amplitude along for PSTM data.

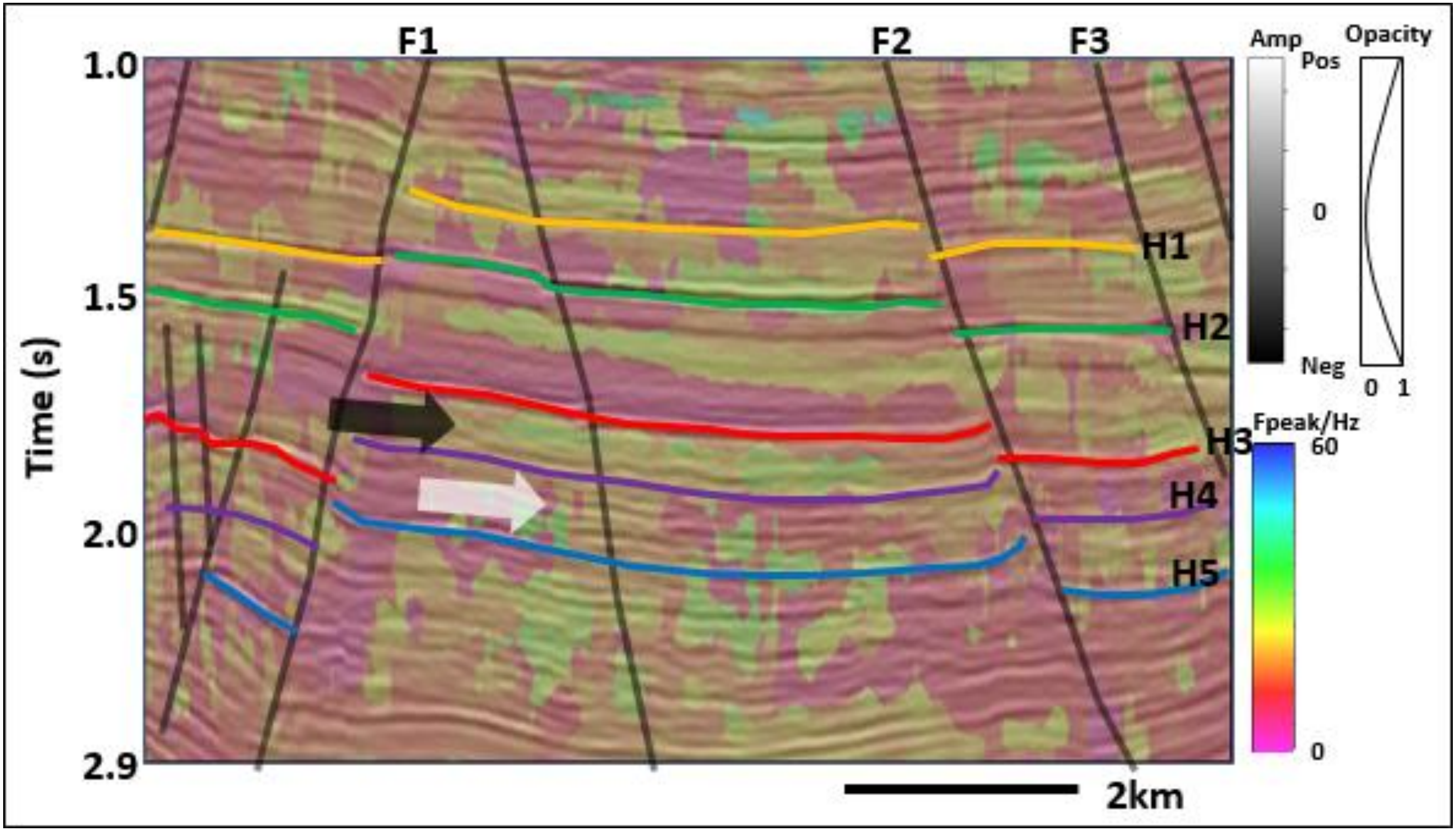

Figure 7. Vertical slice though peak frequency co-rendered with seismic amplitude for PSTM data.

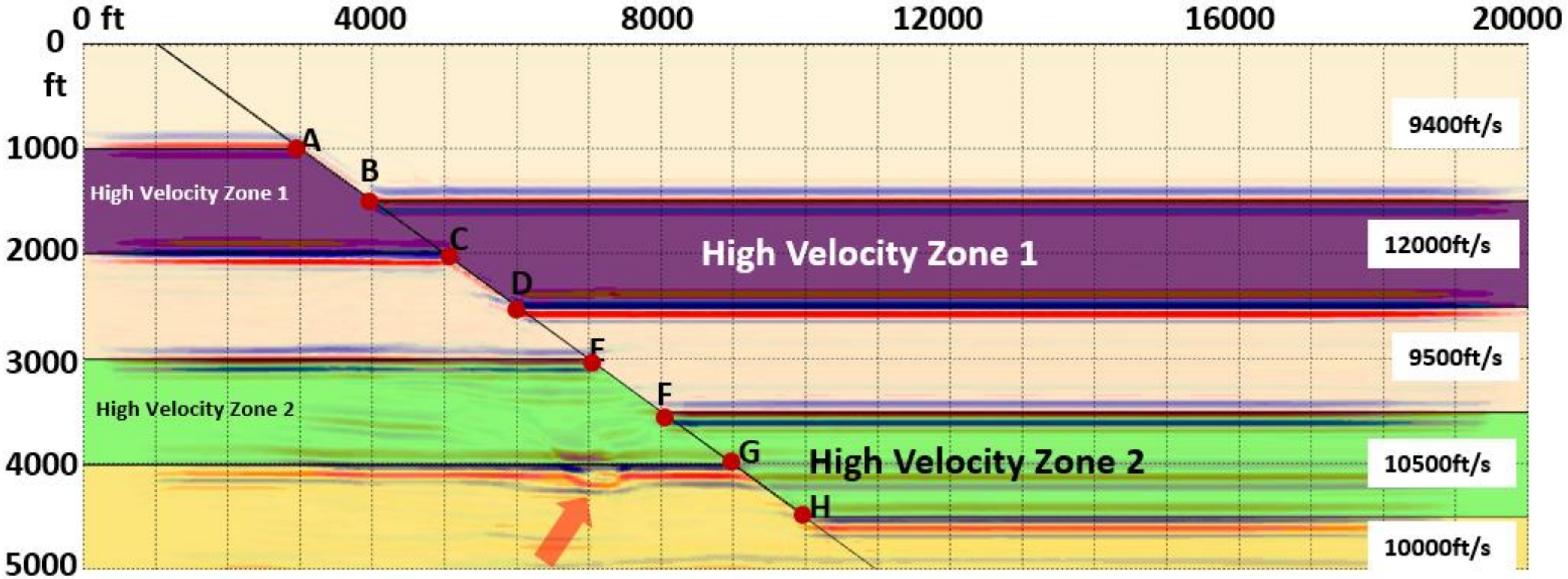

Figure 8. The PSDM seismic profile of the fault model.

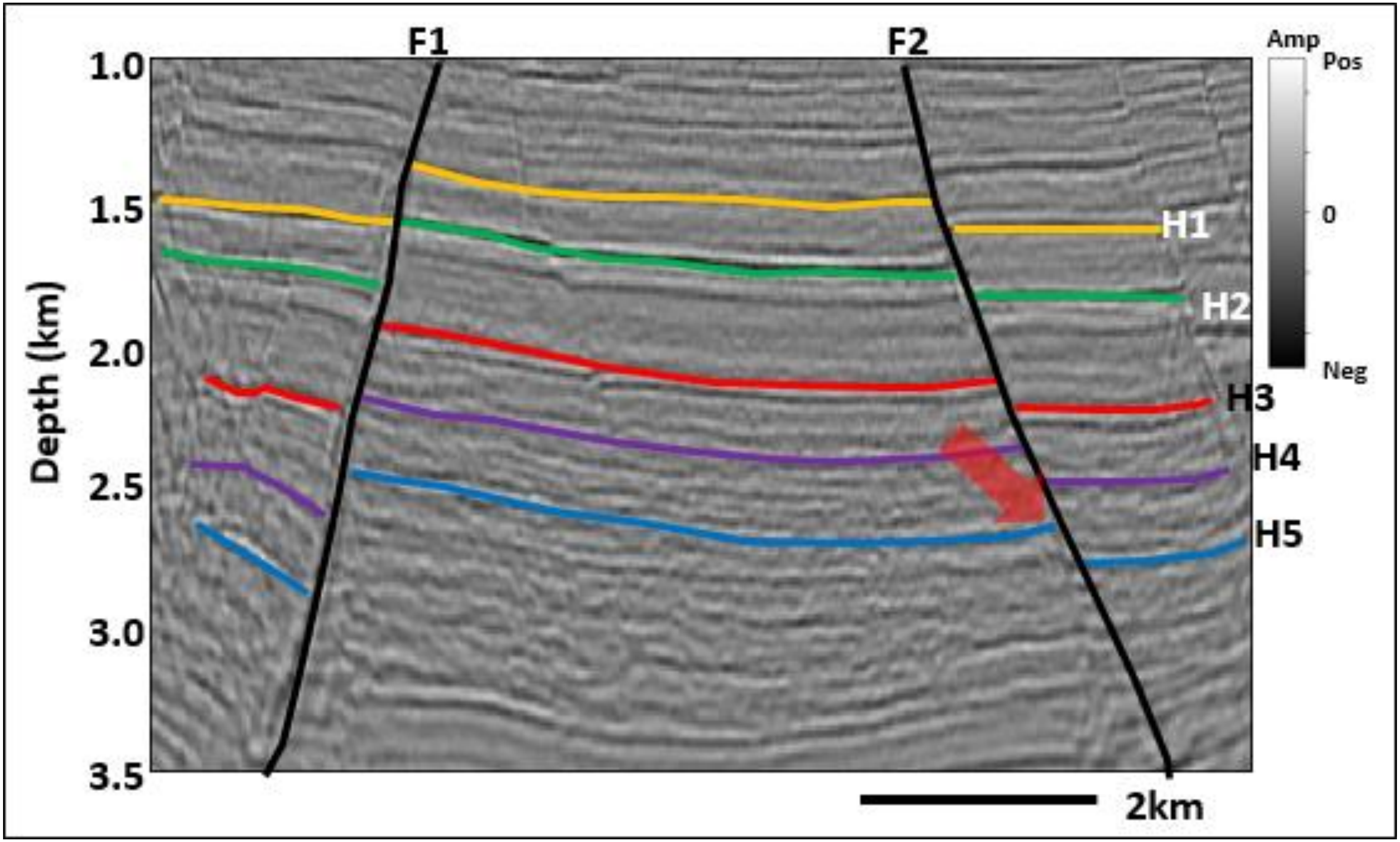

Figure 9. Seismic profile of PSDM amplitude volumes.

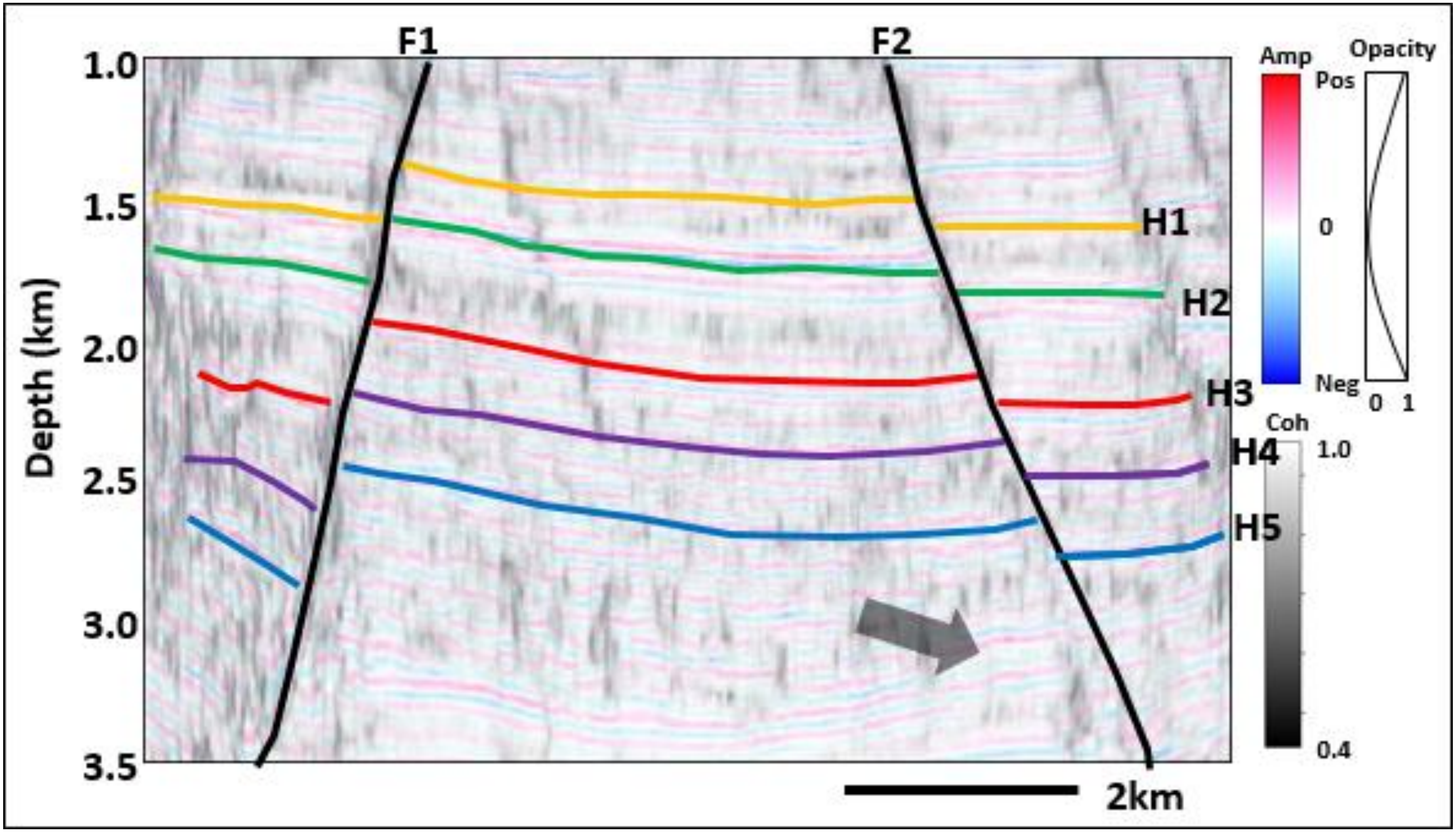

Figure 10. Vertical slice though coherence co-rendered with seismic amplitude for PSDM data.

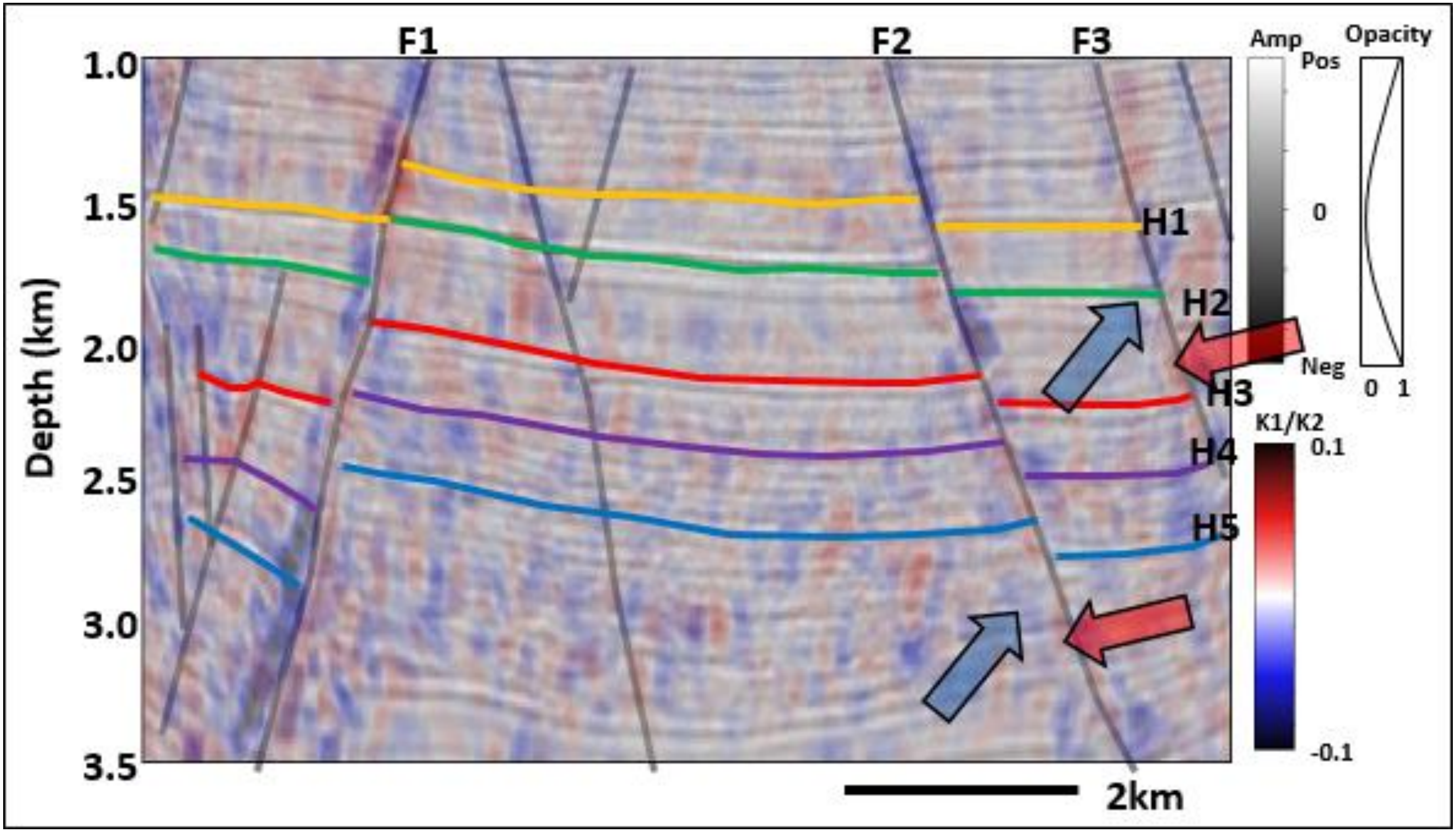

Figure 11. Vertical slice though most positive curvature co-rendered with most negative curvature (with long wavelet) and seismic amplitude along for PSDM data.

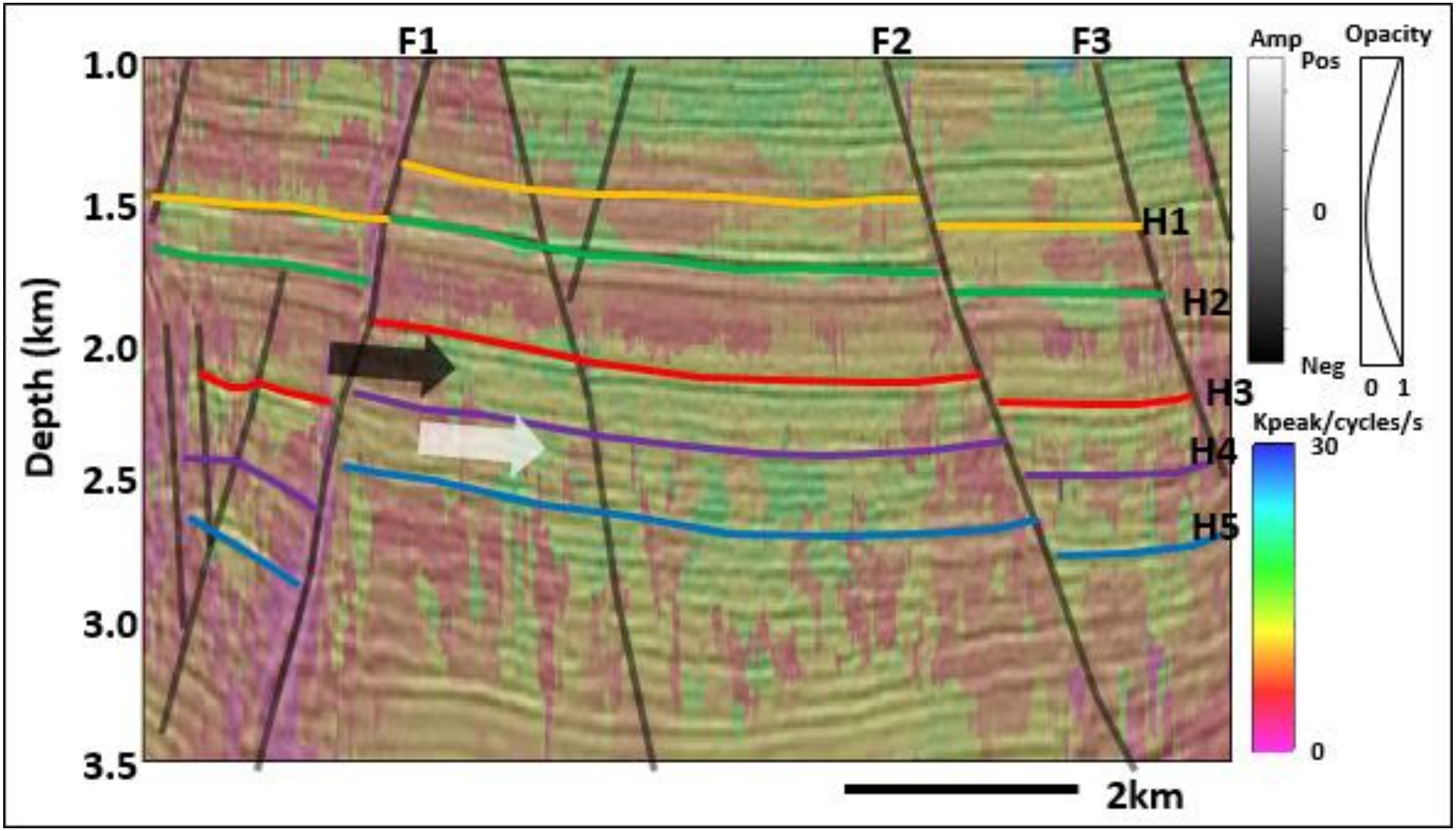

Figure 12. Vertical slice though peak frequency co-rendered with seismic amplitude for PSDM data.

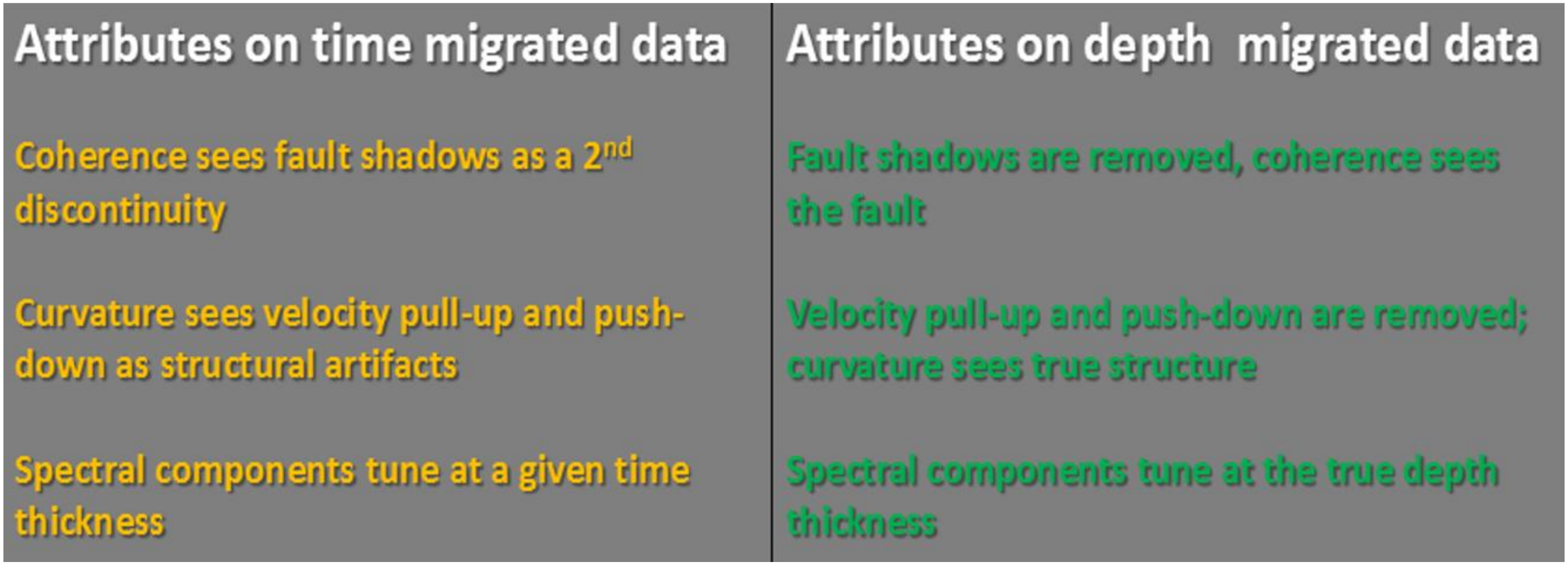

Attributes on time migrated data	Attributes on depth migrated data
Coherence sees fault shadows as a 2nd discontinuity	Fault shadows are removed, coherence sees the fault
Curvature sees velocity pull-up and push-down as structural artifacts	Velocity pull-up and push-down are removed; curvature sees true structure
Spectral components tune at a given time thickness	Spectral components tune at the true depth thickness

Table 1. Attribute comparison of time- vs. depth-migrated data.